International Journal of Trend in Scientific Research and Development (IJTSRD)
Volume 7 Issue 4, July-August 2023 Available Online: www.ijtsrd.com e-ISSN: 2456 – 6470

Modeling of Technologically Hanged Rocks at the Quarry Face

Oluwaseyi A. O., Kutelu B. J., Fakolade O. R.

Department of Mineral and Petroleum Resources Engineering Technology,
Federal Polytechnic, Ado-Ekiti, Nigeria

ABSTRACT

Rock fall is the act of releasing pieces of rock from bedrock slopes provoked by environmental factors, such as physical and chemical weathering, and vibration caused by rock blasting. The evaluation of the rate at which pieces of rock are released from the Quarry's bench face through modeling in order to prevent possible accidents is necessary. The method used for this investigation involves taking field measurements of the slope height, slope angle, length and width of the bench. Rock samples were also taken from the field to the laboratory to carry out tests to determine the density, friction angle and slope roughness of the rock. With this, the models were made with rock fall program. The zone of the Quarry face prune to affectation by Rock fall was predicted to be 15 m from the bottom crest of the IBD Quarry bench face that was occupied by rock pile and 6.5 m for a face without pile. Also, total kinetic, translational and rotational energies of the falling rocks were modeled at different points of the face; the bounce height and end-point were determined.

KEYWORDS: *Rock fall, Quarry face, Bench, End-point, Bounce Height*

How to cite this paper: Oluwaseyi A. O. | Kutelu B. J. | Fakolade O. R. "Modeling of Technologically Hanged Rocks at the Quarry Face" Published in International Journal of Trend in Scientific Research and Development (ijtsrd), ISSN: 2456-6470, Volume-7 | Issue-4, August 2023, pp.229-236, URL: www.ijtsrd.com/papers/ijtsrd57562.pdf

IJTSRD57562

1. INTRODUCTION

Rock fall is the act of releasing pieces of rock from bedrock slopes provoked by environmental factors, such as physical and chemical weathering, and vibration caused by rock blasting or heavy vehicular movement (Schumm and Chorley, 2017; Day *et al*., 2018). Apart from the weathering rates, trigger mechanisms also determine whether Rock fall occurs. Rock fall can be activated in slope by freezing and thawing, geo-structural and seismic activities (Douglas, 2005, Gardner, 2017 and Bull *et al*., 2008). Wieczorek (2015) reported that human activities leading to decreased stability of hill slopes in hard rock and geological factors can also aid rock fall. (Selby, 2016).

Rock fall can occur in different modes, such as freefall, where motion that occurs in the slope gradient is greater than 76° and the translation of the rock and the rotation of the block around its centre were observed (Ritchie, 2010; Azzoni *et al.*, 2012) and air friction can minimally affects the velocity of a freefalling rock (Bozzolo and Pamini 2012). Moreover, at a reduced slope (gradient of about 45^{o}) a bouncing rock gradually transform its movement to rolling (Broilli, 2016). Hungr and Evans (2011) reported that a rolling rock is almost constantly in contact with the slope surface. Other type of motion over the surface of slope is sliding, which generally occurs at the beginning and ending stages of rock fall, the rock will usually stop because of frictional energy (Bozzolo and Panini, 2012). Therefore, the stopping of a falling rock depends on the mean slope gradient, the size of the rock and the material that covers the surface of the slope such as soil, scree and vegetation. Also, small rocks retard more easily than bigger rocks, because the total kinetic energy of small rocks is lower than that of bigger rocks during rock fall, trees can more easily stop small rocks and small rocks retard more easily in depressions between larger rocks on talus slopes (Kirkby and Statham, 2017).

There exist empirical models, process-based models and GIS-based models for the Rock fall analysis. According to Keylock and Domaas (2010) empirical Rock fall models are referred to as statistical models and are based on relationships between topographical factors and the length of the run-out zone of one or more Rock fall events.

Tianchi (2013), carried out 76 major Rock fall test, established inverse logarithmic correlation relationship between the volume of the Rock fall and the ratio of the maximum vertical drop to the maximum horizontal distance travelled. Also the relationship of a positive logarithmic correlation between the volume of the Rock fall and the area covered by the fallen mass was formed. With this, Tianchi (2013) developed a model for an initial estimate of the extent of treating rock fall, if the volume can be estimated. Through comparative study, Moriwaki (2015) found a relationship between the angle of a line connecting the toe with the crown of the rupture, in the first instance, the ratio of the maximum vertical drop to the maximum horizontal distance travelled and, secondly, the landslide volume. Evans and Hungr (2011) on their side, suggest the Fahrböschung principle to forecast run out zones of Rock fall events. The Fahrböschung is the angle between a horizontal plane and a line from the top of a Rock fall source to the stopping point for any given rock fall. The line must follow the fall track of the boulder. On the other hand, Evans and Hungr (2011) suggested the minimum shadow angle as an alternative principle. It is the angle of a straight line between the peak point of the talus slope and the stopping point of the longest run out boulder. After investigating 16 talus slopes in British Columbia Evans *et al*., (2018) reported a minimum shadow angle of 27.5° which should only be used for a first approximation of the length of a Rock fall run out zone. Keylock and Dommas (2010) used Rock fall data to test three empirical models on their ability to predict the maximum length of Rock fall run out zones using simple topographic parameters.

Process-based models describe the modes of motion of falling rocks over slope surfaces. Kirkby and Statham (2017) created a process based Rock fall model for transport of rocks that slide over slopes surface. This model calculated the velocity of the falling rock at the base of the cliff with the following expression:

$$v = 2g \times h \quad \text{..... (equation 1)}$$

Where:
v: velocity (ms^{-1});
g: acceleration due to gravity (ms^{-2}) and
h: fall height (m).

Based on this velocity, the component of the fall velocity parallel to the slope surface was calculated, assuming that this component of the velocity is being conserved during the first impact of the rock on the slope surface. Then, the stopping position was calculated by the ratio of the fall velocity and a frictional force, which was determined by the dynamic angle of friction. Keylock and Domaas (2010) developed the simple dynamics Rock fall model, which is a process-based model based on the model of Kirkby and Statham (2017). The simple dynamics Rock fall model was tested using Rock fall data presented by Domaas (2008). Their model calculated the travel distance over the slope surface on the basis of the friction force according to Kirkby and Statham (2017) and the acceleration due to gravity. On the basis of calculated probabilities of modeled Rock fall travel distances, Keylock and Domaas (2010) concluded that the simple dynamics Rock fall model did not appear to hold a significant advantage over the empirical models tested in their study. In addition to the models of Kirkby and Statham (2017) and Key lock and Domaas (2010), there is a large group of process-based models that are rather similar (Wu, 2000; Bozzolo and Pamini, 2012; Evans and Hungr, 2011; Bozzolo et al., 2015; Azzoni et al., 2012, Chau et al., 2017). Three factors correspond in all these models. First, these process-based models are two-dimensional slope-scale models that restricted falling boulders to move in a vertical plane. Consequently, lateral movements were not simulated. Secondly, the Rock fall track was defined as a composite of connected straight lines with a slope angle equal to the measured mean slope gradient on the represented segment of the Rock fall track as visualized. Finally, motions were simulated as a succession of flying phases and contact phases. The flying phase was simulated with a parabola equation based on the initial velocity in two directions and the acceleration due to gravity. The collision point of the rock on the slope surface was calculated with the intersection of the parabolic flying function and the straight slope segments. The first difference between these two-dimensional process-based models is that some of these models considered a falling rock with its mass concentrated in one point (Bozzolo and Pamini, 2012; Kobayashi and Cruden M.D 2018; Evans and Hungr, 2011; Azzoni *et al.*, 2012), while other models considered bouncing, rolling and sliding as identical movements that can be described by a succession of impacts and bounces (Bozzolo *et al*., 2015; Pfeiffer and Bowen, 2015). Models applying specific algorithms for calculating rolling and sliding velocities mainly used Coulomb's law of friction,

$$F_f = \mu_f . m . g . \cos\theta \quad \text{equation 2}$$

Where,
F_f is friction force (tangential to the slope surface) (kg/ms^{-2})
μ_f is coefficient of friction;
m is mass of the rock (kg);
g is acceleration due to gravity (ms^{-2});

Θ is mean slope gradient (°).

The calculated friction force could then be used for calculating the sliding or rolling velocity of a rock after displacement over a given distance over the slope surface (Bozzolo and Pamini, 2012; Dijke and Westen, 2013; Kobayashi and Cruden M.D 2018; Evans and Hungr, 2011; Azzoni *et al*., 2012). Here, the friction coefficient is the most determining factor for the velocity.

GIS-based models are those either running within a GIS environment or they are raster based models for which input data is provided by GIS analysis. GIS-based Rock fall models consist of three procedures. The first procedure identifies the Rock fall source up areas in the region of interest, the second determines the fall track and the third calculates the length of the runout zone (Hegg and Kienholz, 2016). Meissl (2014) developed two GIS-based Rock fall models using an empirical model for calculating the runout zone. The first model was Schattenwinkel. This model was based on the minimum shadow angle principle (Evans and Hungr, 2011). The second model of Meissl (2014) was called Geometrische Gefälle. This model was based on the angle of the shortest line between the top of the Rock fall source scar and the stopping point. Apart from these principles both models were identical, since both models used an identical module for calculating the fall track and the source areas (Callaghan and Mark, 2013; Meissl, 2014). In a GIS-based distributed Rock fall model the terrain is represented by multiple rasters, which are derived from GIS data layers. Each raster represents a certain property of the terrain. Dijke and Westen (2013) developed a distributed model that performs a neighborhood analysis to a DEM derived from an isocline map with an equidistance of 20 m, representing an area of 80 km^2. A neighborhood analysis calculated the fall direction for each raster cell. The direction was determined towards the neighboring cell with the minimum height value. The velocity calculation of the model was based on an energy conservation principle as described by Scheidegger (2012). On the basis of this principle the velocity of the falling rock was calculated following,

$$V = V_o + 2g.\left(h - \mu_f + 4x\right) \quad equation\ 3$$

Where, V is velocity of the falling rock (ms^{-1});

V_0 is initial velocity of the falling rock (ms^{-1});

g is acceleration due to gravity (ms^{-2});

h is fall height (m);

μ_f is coefficient of friction;

X is distance travelled over the slope surface (m).

The velocity was calculated for each raster cell within the fall track, starting at a potential Rock fall source cell. Potential Rock fall source cells were defined by the mean slope gradient (>60°) and the value of the friction coefficient (μ_f) depended on the soil cover type. Dijke and Westen (2013) concluded that their model was able to compute the general distributions of Rock fall areas shown on their maps. The GIS-based distributed model of Meissl (2014) was called Sturzgeschwindigkeit and simulated two different modes of motion: freefalling and sliding. Meissl (2014) concluded that the simulated Rock fall patterns on high altitudinal zones generally correspond with the mapped patterns, but unfortunately no model accuracies were given.

2. STUDY AREA

This study was carried out in IBD Impex limited Quarry, Afao, Ekiti state, located in longitude 5°19'32" E and latitude 7°42'25"N.

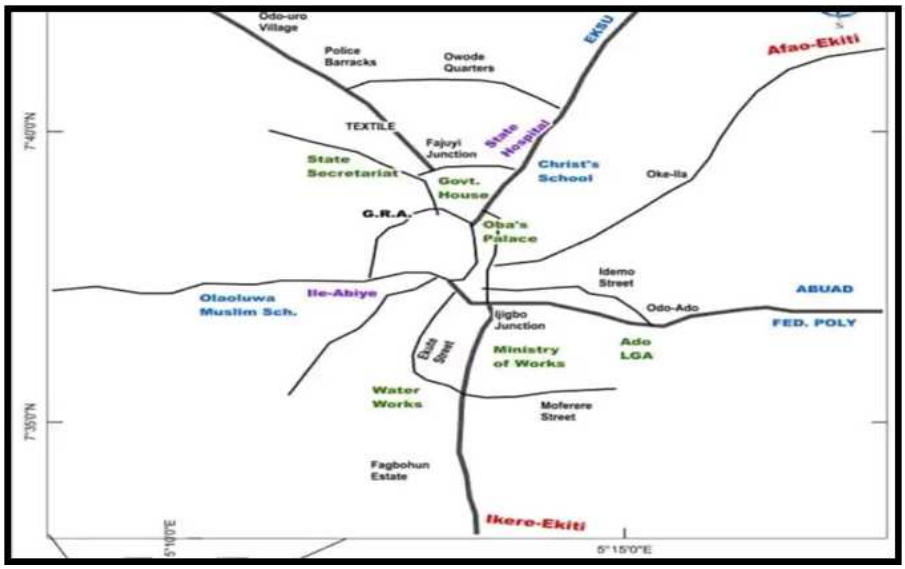

Fig 1 Location Map of IBD Impex limited, Afao, Ekiti State, Nigeria (https://www.google.com)

3. MATERIALS AND METHODS

The Quarry bench height was measured and the width was measured from the bottom crest of the bench under investigation to the top crest of the following bench. Also, slope angles for both quarries were determined by equation 4:

$$Slope\ Angle = Tan^{-1}\left(\frac{Vertical\ distance}{Horizontal\ distance}\right)\ equation\ 4$$

And the slope distance by equation 5

$$Slope\ distance, L = \frac{Bench\ Height, H}{sin\theta}\ , where\ \theta = \ angle\ of\ bench\ slope\ equation\ 5$$

In order to estimate the weight of rock that will likely fall from the quarry face, density of the rock was determined in the laboratory by taking ten samples of intact rocks from the quarry site in a random manner, weight and of each sample was measured, then the measuring cylinder was filled with water to the desired level and the reading, V_0, was taken as initial volume. Separately, each of the rock samples was dipped inside of the cylinder and the reading V_1, as the final reading. The volume change was determined by the following relation:

$$\Delta V = V_1 - V_o\ equation\ 6$$

The average density of the sample was calculated by the expression in equation 7:

$$Average\ density = \frac{\sum_{i=1}^{n} weight\ of\ samples}{\Delta V}\ equation\ 7$$

Then the size of the likely boulders that can fall were estimated by measuring the length of the protruded edges of the piece of the rock, its volume was determined and consequently the weight of the possible falling rock was calculated by multiplying the density by the determined volume. Then the volume of the rock was multiplied with specific gravity to get the weight of the rock.

$$Rock\ weight = V_r.SG_r\ equation\ 8$$

Where, V_r is the volume of the rock

SG_r is the specific gravity of the rock

3.1. MODELING

The input parameters used modeling the rock fall at the face of the quarry are: angular velocity, coefficient of normal restitution, slope roughness, friction angle and coefficient of tangential restitution. In this study, the initial velocity is taken to be cero, because at this point the movement of the rock is very slow. On the other hand, the coefficient of normal restitution (R_N) and tangential restitution (R_T) were taken from the literature according to the case study of the rock that is similar to the rock under study, that is, R_N= 0.35 and R_T = 0.83.

The Rock fall was modeled with the Rocfall program using the parameters measured which are slope height, slope angle, rollout distance and elevation of the rock. The slope was first created, the slope materials were defined and materials were assigned to the slope segments. The slope roughness was determined by tracing a straight a line of 1 m along the wavy face of the rock slope under study. The angle of inclination of the wavy line was measured at several points by sampling a normal distribution. The mean of the distribution which is equal to the original slope segment inclination and the standard deviation were calculated.

4. RESULTS AND DISCUSSION

Figure 1 shows the face of bench slope of IBD Implex Limited, revealed poor blasting operation, there appeared dangerously hanged intact rocks which could be unsafe to the loading and transportation crews due to possibility of rock fall. IBD quarry is largely made of granite rock.

Plate 1. Face of the bench, IBD Impex, Limited, Afao, Ekiti State, Nigeria.

The data used to estimate the modeling of the rocks that were thrown are shown in Table 1 and Table 2.

Table 1 Modeling data for IBD Impex, Limited

Density of rock (t/m^3)	Volume of Rock fall (m^3)	Mass of Rock fall (kg)	Height of bench (m)	Width bench (m)	Bench slope angle (^{o})	Friction angle (^{o})	Coef. of normal restitution	Standard Deviation	Coef. of tangential restitution	Standard Deviation	Horizontal velocity	Slope roughness (^{o})
2.79	2.64	7.4	12	15	90	37	0.35	0.04	0.83	0.04	1.5	4.6

Table 2 Vertices of the IBD Impex limited quarry bench

S/N	X(m)	Y(m)
1	0	398
2	15	398
3	15	387
4	30	387

The modeled face with blasted pile were shown in figure 2a and 2b with waving down sloping which is due to the zigzag positioning of the blasted rocks. When throw occurs, the seeder rock may likely hit any of the pointed area of the rock pile and this dynamism could change the direction of the seeder, cause the bounce height and end-point location to increase, even, the throw velocity could be made higher, thereby increasing the seeder throw energy. In this study, the bounce height of 0.5 m was recorded at the location 5 m from the bench lower crest, 1 m at location 10 m and from location 11.5 to 14 m, the bounce height ranges between 0.5 to 0.9 m. On the other hand, the rock end-point, where it finally came to a stop was 15 m from the bottom crest of the bench height (figure 2b).

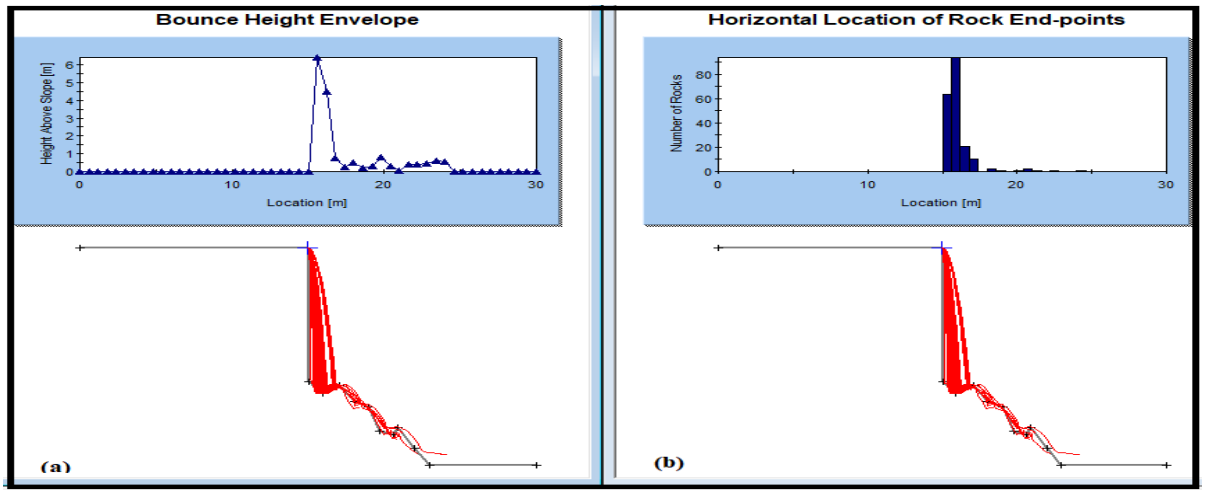

Fig. 2 The modeled IBD quarry bench face with the graph of bounce height and rock end point

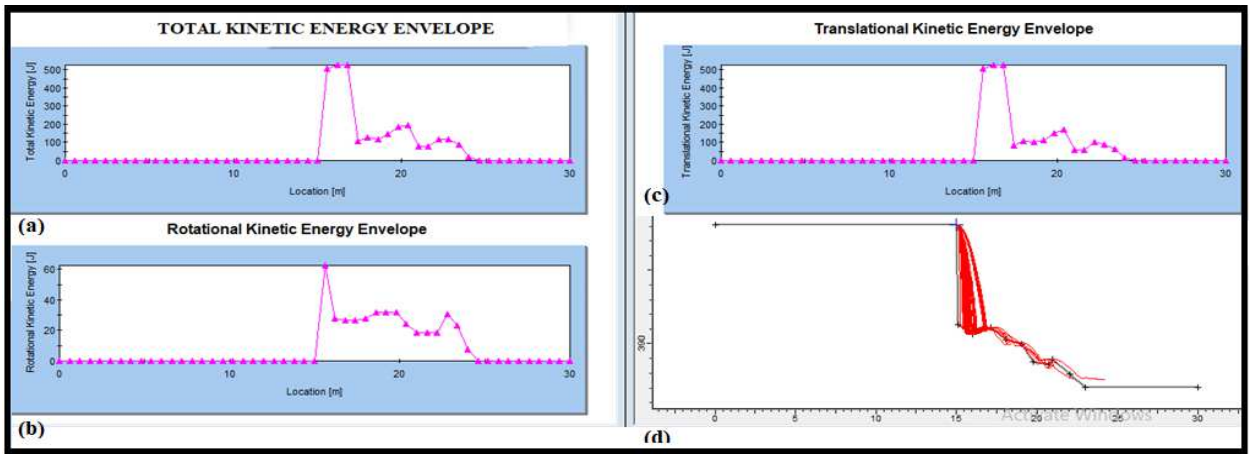

Fig. 3 The modeled IBD quarry face with the graph of the types of energies displayed

Also, figures 3a, b, c, show different energies with which the rocks thrown were travelling: total kinetic energy was highest (900 J) at the initial point when seeder was released. As the rocks travelled the kinetic energy got reduced to 100 J at the location, 4 m from the bottom crest of the quarry bench, then it increased to 200 J at location 10 m and again descended to 60 J at 11 m, ascending to 100 J at 12 m and finally the kinetic energy got reduced to zero at 15 m; the rotational and translational energies follow the same waving pattern which range between 15 to 25 J within location 1 to 27 m, and between 50 to 500 J within 10 m from the lower crest of the bench respectively. The unstable manifestation of the energies was due to the waving nature of the rock mass pile at the quarry face.

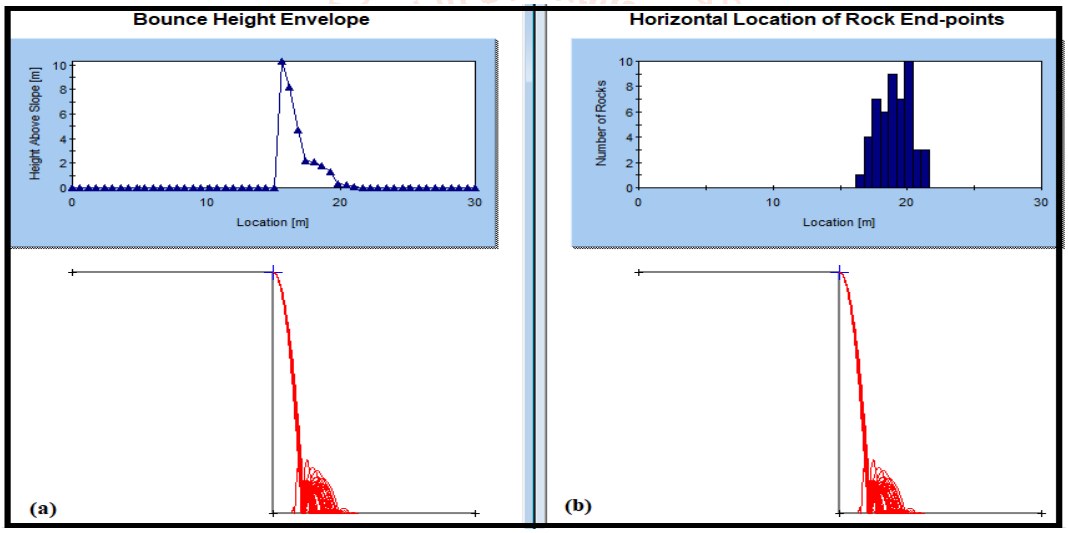

Fig.4. the rock throws bounce height and end-points at the face without rock pile.

Moreover, figure 4a and b shows that the bounce height was at its maximum of 0.2 m at the 5 m location measuring from the quarry face and the end-point was at 6.5 m from the lower crest of the quarry face.

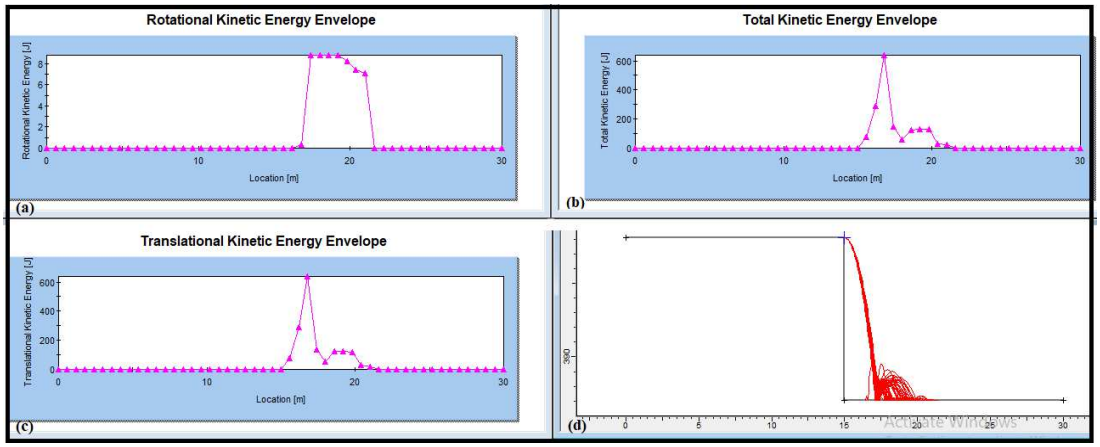

Fig. 5 The modeled IBD quarry face without rock pile and its graph of energy types.

In Mine design, safety of workers and equipment is paramount, especially during operations at the quarry face. In the light of this study, the end-point values will help to determine the distance that is safe for workers to stand

and the various types of energies determined will help to measure the impact of the Rock fall on the objects. When the quarry operations are to take place within lesser distance, protection must be provided against possible rock fall and the operation equipment must be constructed with integrity that is strong enough to arrest the destruction of the same by rock fall. In IBD Quarry, considering the height of Rock fall (10 m) analyzed, the end-point of 15 m means that the safe place for workers and equipment is any distance beyond 15 m from the bottom crest of the Quarry when rock pile is still on the face site and beyond 6.5 m in the case where the face is free of rock pile. Also, with the knowledge of the energy of the rock fall, the likely impact can be estimated and the design of the equipment could be such that the effect of the impact would be reduced to bearable minimum.

5. CONCLUSIONS

In this study, the zone of the Quarry face prune to affectation by Rock fall was predicted to be 15 m from the bottom crest of the IBD Quarry bench face with rock pile and 6.5 m for a face without pile. Also, total kinetic, translational and rotational energies of were modeled at the different points of the face; the bounce height and end-point were determined.

5.1. RECOMMENDATION

This study is recommended for the Open Pit Mine project design department of Mining Industries. But caution should be made to carry out all necessary process of data collection and laboratory test according to Industrial standard before application.

REFERENCES

[1] Azzoni, A., Barbera, G.L. and Zaninetti, A. 2012: Analysis and prediction of rock falls using a mathematical model. International Journal of Rock Mechanics and Minin Ltd, 405–35.

[2] Bozzolo, D. and Pamini, R. 2012: Simulation of rock falls down a valley side.

[3] Bozzolo, D., Pamini, R. and Hutter, K. 2015: Rock fall analysis – a mathematical model and its test with field data. Proceedings of the 5thInternational Symposium on Landslides in Lausanne, Rotterdam: Balkema, 555–60.

[4] Broilli, L. 2016: Ein Felssturz in Großversuch. Rock Mechanics Suppl. 3, 69–7.

[5] Bull, T., Kasa, A. And Taha, M.R., 2008. Fuzzy logic system for slope stability prediction, International Journal on Advanced Science Engineering Information Technology, 2, 38–42.

[6] Callaghan, T.J., and Mark, T.D., 2013: Computer Simulation of Rock falls. Bulletin of Association of Engineering Geologists, Vol. 26, No. 1. pp135 -146

[7] Chau, W.B., King, J., Kong, F.C., Moutoux, T. and Phillips, W.M. 2017: Lichen dating of coseismic landslide hazards in alpine mountains. Geomorphology 10(1), 253–64.

[8] Day, R. W., Chen, H., Chen, R. and Huang, T.2018: An application of an analytical model to a slope subject to rock fall. Bulletin of the Association of Engineering Geologists 31(4), 447-58.

[9] Dijke, K., and Westen, H., 2013. Effects of geologic factors on Rock fall events: Ermenek (Karaman), Turkey. EGU General Assembly 2008, Wien, Austria, Abstract No. EGU2009-A-2882.

[10] Douglas W.B., 2005. Rock falls. In: Brunsden D, Prior DB Slope stability. Wiley, New York, pp. 217–256.

[11] Domaas J.P. 2008: Rock temperature measurements in two alpine environments: implications for frost shattering. Arctic and Alpine Research 21, 399–416.

[12] Evans S.G, and Hungr O., 2011. The assessment of Rock fall hazard at the base of talus slopes. Canadian Geotechnical Journal, 30, 620–636.

[13] Evans, F., Magnier, S.A., Montani, S. and Descoeudres, F. 2018: Numerical study of rock block impacts on soil-covered sheds by a discrete element method, 5ème Conférence Nationale en Génie Parasismique, AFPS'99, Cachan.

[14] Gardner, T.C. 2017: Rock fall control in Washington State, Rock fall prediction and control and landslide case histories. Transportation Research Record 1343, 14–19

[15] Hegg, H. and Kienholz, P. 2016: Assessment geomorphic hazards and priorities for forest management on the Rigi north face, Switzerland. Mountain Research and Development 14(4), 321–28.

[16] Kirky M.D. and Statham, J.D. 2017: Landslide types and processes. In Turner, A.K. and Schuster, R.L., editors, Landslides: investigation and mitigation. Washington DC: Transport Research Board, 36–75.

[17] Keylock, C. and Domaas, U. 2010: Evaluation of topographic models of Rock fall travel

distance for use in hazard applications. Arctic, Antarctic, and Alpine Research 31(3), 312–20

[18] Kobayashi, R.W. and Cruden M.D 2018: Case studies of Rock fall in soft versus hard rock. Environmental and Engineering Science 32, 709–2Geoscience 3(1): 133–40.

[19] Meissl, G. 2014: Modellierung der Reichweite von Felsstürzen. Fallbeispeile zur GIS gestützten Gefahrenbeurteilung aus demBeierischen und Tiroler Alpenraum. Innsbrucker Geografischen Studien 28. Ph.D.Thesis, Universität Innsbruck, Innsbruck, 249 pp.

[20] Moriwaki, H., 2015. Geomorphological prediction of the travel distance of a debris. The China–Japan field workshop on landslide. Xian Lanzhou, China, 79–84.

[21] Pfeiffer, F. and Bowen, T. 2015: Three-dimensional dynamic calculation of rock falls, In Herget, G. and Vongpaisal, S., editors, Proceedings of the Sixth International Congress on Rock Mechanics. Montreal. Rotterdam: Balkema, 337–42.

[22] Ritchie, A.M. 2010: Evaluation of Rock fall and its control. Highway Research Record 17, 13–28.Washington, DC: Highway Research Board, National Research Council.

[23] Rocscience 2002. Rocfall software—for risk analysis of falling rocks on steep slopes. Rocscience user's guide

[24] Scheidegger, S.G 2012: The assessment of Rock fall hazard at the base of talus slopes Canadian Geotechnical journal 30, 620-36

[25] Selby T.H 2016: Flowing, rolling, bouncing, sliding, synopsis of basic mechanisms, Acta mechanical 64, 101-10.

[26] Statham, F. and Bowen, G. 2015: Numerical study of rock block impacts on soil-covered sheds by a discrete element method, 5ème Conference Nationale en Génie Parasismique, AFPS'99, CacDouglas, G.R. 2015: Magnitude frequency study of Rock fall in Co. Antrim, North Ireland. Earth Surface Processes and Landforms 5, 123–29.

[27] Schumm, J.S and Chorley J.R. 2017: Rock fall frequency and distribution in the Highwood Pass area, Canadian Rocky Mountains. Zeitschrift für Geomorphologie 27(3), 311–24.

[28] Tianchi, L. 2013: A mathematical model for predicting the extent of a major rock fall. Zeitschrift für Geomorphologie 27(4), 473–82

[29] Wiezoneck E.M. 2015: Simulating landslides for natural disaster prevention. In Arnaldi, B. and Hegron, G., editors, Computer animation and simulation '98.

[30] Wu M.D. 2000 Terrain analysis and distributed modelling in hydrology.